# Effect of Fe substitution on magnetocaloric effects and glass-forming ability in Gd-based metallic glasses

Lin Xue[a,b], Jun Li[a,b], Weiming Yang[c], Chenchen Yuan[a,b], Baolong Shen[a,b,c,*]

[a] School of Materials Science and Engineering, Southeast University, Nanjing 211189, China
[b] Jiangsu Key Laboratory for Advanced Metallic Materials, Nanjing 211189, China
[c] Institute of Massive Amorphous Metal Science, China University of Mining and Technology, Xuzhou 221116, China

## ARTICLE INFO

## ABSTRACT

In this work, we report on the systematic variation of the glass-forming ability (GFA) and magnetocaloric effect (MCE) in $Gd_{55}Co_{20-x}Al_{24}Si_1Fe_x$ (x = 0, 1, 2, 3, 4 and 5 at%) metallic glasses (MGs), which are potential candidates for magnetocaloric cooling applications. The addition of Fe broadens the full width of half maximum of magnetic entropy change ($\delta T_{FWHM}$), thereby greatly increases the refrigeration capacity (RC). Accordingly, the $\delta T_{FWHM}$ as large as 118 K, magnetic entropy change $|\Delta S_M|$ of 7.26 J kg$^{-1}$K$^{-1}$ at 130 K, and corresponding large RC of 857 J kg$^{-1}$ under applied field of 5 T are obtained for the composition with 5 at% Fe substitution. By increasing the atomic fraction of Fe dopants, the Curie temperature $T_C$ increases systematically at the same time. Such high GFA of novel Gd-based MGs with large MCE makes them attractive candidates for magnetic refrigeration applications in the future.

## 1. Introduction

Magnetic refrigeration based on magnetocaloric effect (MCE), due to its great merits such as environmental friendliness and relatively high efficiency, has been regarded as a potential alternative to replace the conventional gas compression/expansion refrigeration [1–4]. Until now, several intermetallic compounds, such as Gd-Si-Ge [5], La-Ca-Mn-O [6], Ni-Mn-Ga [7], La-Fe-Si [8], Mn-Fe-P-As [9], Ni-Mn-Sn [10], etc., display giant MCE due to their first order magneto-structural phase transitions. However, for crystalline materials with large magnetic entropy change ($|\Delta S_M|$) related to a first-order magnetic transition, magnetic hysteresis as well as heat hysteresis alongside of the refrigeration cycle is inevitable. Even for crystalline materials with a second-order magnetic transition that have no hysteresis, they usually possess lower refrigeration capacity (RC) due to narrow full width at half maximum of $|\Delta S_M|$ ($\delta T_{FWHM}$) [11]. In contrast, a relatively large $|\Delta S_M|$ and $\delta T_{FWHM}$ are often available in glassy materials with a second-order magnetic transition, which result in a larger RC [12]. As excellent glassy materials, Gd-based glassy alloys, unlike traditional crystalline materials in which the constituent atoms reside at thermodynamic equilibrium, are metastable materials in far-from-equilibrium states [13,14]. They have additional characteristics that are desirable for magnetic refrigerants: extraordinary tunability of the transition temperature by alloying [15,16], good mechanical properties [17] and negligible magnetic

hysteresis, etc. Moreover, the fact that these amorphous materials display negligible magnetic anisotropy fundamentally simplifies the study of their magnetic transition, making them a good testing ground for analyzing the physics behind the MCE and for developing thermodynamic models to represent their response [18]. An active magnetic regenerator system requires large MCE and plates-shaped or spherical particles with an optimal geometry to achieve the best thermal transport properties between magnetic refrigerants and heat-exchange medium [19]. Therefore, the low glass-forming ability (GFA) of Gd-based bulk metallic glasses (BMGs) has hindered their development seriously for a long time [20]. Generally speaking, enhanced GFA inevitably leads to the deterioration of MCE. It is an enormous challenge to develop excellent GFA of Gd-based BMGs with large MCE [21].

In this work, with the aim of preparing large MCE Gd-based BMGs with excellent GFA, the effect of Fe addition on the performance in Gd-Co-Al-Si BMGs was investigated. It is found that the addition of only 1 and 2 at% Fe can efficiently improve the GFA of $Gd_{55}Co_{20}Al_{24}Si_1$ BMG. Meanwhile, the RC and the Curie temperature ($T_C$) of $Gd_{55}Co_{20-x}Al_{24}Si_1Fe_x$ MGs are effectively improved. The derived conclusions provide a compelling approach for manufacturing Gd-based BMGs with excellent GFA and large MCE.

* Corresponding author. School of Materials Science and Engineering, Southeast University, Nanjing 211189, China.
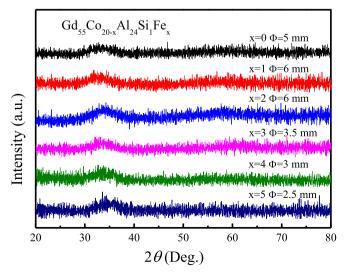E-mail address: blshen@seu.edu.cn (B. Shen).

## 2. Experimental

The alloy ingots with nominal compositions of $Gd_{55}Co_{20-x}Al_{24}Si_1Fe_x$ (x = 0, 1, 2, 3, 4 and 5 at%) were prepared by arc-melting a mixture of pure Gd, Co, Al, Si and Fe under high purity argon atmosphere. The purities of the raw elements are better than 99.9 wt%. Ribbons with a width of 1 mm and a thickness of approximately 33 μm were produced by the single-roller melt spinning method, and rods with diameter of 1–7.0 mm were prepared by copper mold casting technology. Thermal analysis was carried out by differential scanning calorimetry (DSC, NETZSCH 404 F3) with a constant heating rate of 40 K/min under purified argon atmosphere. The data of glass transition temperature ($T_g$) and onset crystallization temperature ($T_x$) of were determined from the thermal analysis traces with an accuracy of ± 1 K. Microstructure was examined by X-ray diffraction (XRD, Bruker D8 Advance) with Cu $K\alpha$ radiation. The magnetic properties of glassy ribbons were measured by a SQUID magnetometer (MPMS, Quantum Design R). Temperature dependence of magnetization (M-T) curves of the amorphous ribbons were measured from 4 to 260 K under an applied field of 200 Oe, the isothermal magnetization (M-H) curves of the ribbons were measured from 4 to 220 K with a field change of 0–5 T.

## 3. Results

Fig. 1 shows the XRD patterns of as-cast $Gd_{55}Co_{20-x}Al_{24}Si_1Fe_x$ (x = 0, 1, 2, 3, 4 and 5) rods. No sharp peaks can be seen in Fig. 1, and only two broad diffusion peaks locate at 35° and 58°, confirming their fully amorphous states. Surprisingly, cylindrical rods with diameter of 6.0 mm for compositions with 1 and 2 at% Fe addition are still full of amorphous structure. It means that a minor Fe addition improves the GFA in this Gd-based BMG. However, the critical diameter decreases rapidly as the further addition of Fe.

Fig. 2 displays the DSC curves of as-cast $Gd_{55}Co_{20-x}Al_{24}Si_1Fe_x$ (x = 0, 1, 2, 3, 4 and 5) BMGs. No obvious change of the $T_g$ was found with Fe addition. The $T_g$ is near 595 K, followed by several crystallization exothermic peaks above 660 K. The $T_x$ moves toward lower temperature with the increase of Fe doping. The $\Delta T_x$ was extended to as large as 74 K, and the $\Delta T_x$ of the alloys were at least 63 K with more Fe addition as listed in Table 1, which are much larger than most of reported glassy alloys [22,23]. The large $\Delta T_x$ of the glassy system indicates the probable excellent GFA, which is associate with the XRD results.

Fig. 3 shows the temperature dependence of the magnetization of the as-spun $Gd_{55}Co_{20-x}Al_{24}Si_1Fe_x$ (x = 0, 1, 2, 3, 4 and 5) ribbons. The
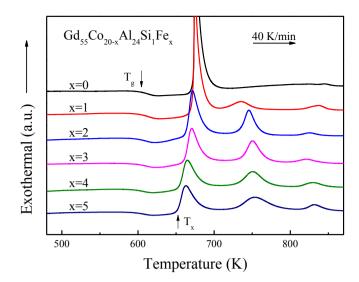
**Fig. 2.** DSC curves of $Gd_{55}Co_{20-x}Al_{24}Si_1Fe_x$ bulk metallic glasses.

data were acquired under an applied magnetic field of 200 Oe. As the temperature increases, the magnetization decreases; this decrease results from the magnetic transition of the alloys from a ferromagnetic state to a paramagnetic state. Defined as the temperature of the maximum value of $|dM/dT|$, $T_C$ for compositions with x = 0, 1, 2, 3, 4 and 5 are determined to be 100, 107, 111, 117, 121, and 126 K, respectively. It is clear that the $T_C$ increases as the Fe content increases.

The hysteresis loops of $Gd_{55}Co_{20-x}Al_{24}Si_1Fe_x$ (x = 0, 1, 2, 3, 4 and 5) glassy ribbons were measured at 5 K under a field of 5 T as show in Fig. 4. For all the samples, the enlarged part of the curves near zero magnetic field present excellent soft magnetic properties with negligible hysteresis and very small coercivity, which can be attribute to the weak magnetic anisotropy resulting from the structural disorder [24]. The saturation magnetizations ($M_S$) are 184, 175, 185, 190, 191 and 192 emu/g for $Gd_{55}Co_{20-x}Al_{24}Si_1Fe_x$ glassy ribbons with x = 0, 1, 2, 3, 4 and 5, respectively, at a magnetic field above 1000 kA/m.

Fig. 5 (a) shows the variation of the magnetization as a function of the applied magnetic field at different temperatures for $Gd_{55}Co_{20-x}Al_{24}Si_1Fe_x$ (x = 0, 1, 2, 3, 4 and 5) glassy ribbons. As shown in Fig. 5 (a), below the $T_C$, the magnetization curves increase abruptly at a rather low field and rapidly saturate; this rapid saturation suggests that these alloys show prominent ferromagnetic behaviors. Above the $T_C$, the increase of the magnetization curves is nearly linear with the magnetic field; this behavior suggests that the samples have the characteristics of paramagnetism. Fig. 5 (b) presents the corresponding Arrott plots that calculated from the isothermal magnetization curves in Fig. 5 (a). According to Banerjee criterion [25], a magnetic transition is considered as first-order when the slope of Arrott plot is negative; otherwise, it is expected to be second-order when the slope is positive. It can be found all slopes in Fig. 5 (b) remain positive without inflection point, it illustrates that the Gd-based alloys in this work undergo a second order phase transition from ferromagnetic to paramagnetic states. This character manifests the negligible thermal hysteresis and reduced magnetic hysteresis in these alloys and demonstrates a beneficial characteristic for the magnetic refrigeration application.

The magnetic entropy, which is associated with the MCE, can be calculated from the isothermal magnetization curves in Fig. 5 (a) as a function of magnetic field. According to the classical thermodynamic theory [26], the magnetic entropy change produced by the variation of a magnetic field from 0 to $H_{max}$ is given by

$$\Delta S_M(T, H) = S_M(T, H) - S_M(T, 0) = \int_{H_0}^{H_{max}} \left( \frac{\partial M}{\partial T} \right) dH \tag{1}$$

where $H_{max}$ and $H_0$ represent the maximum and 0 value of the magnetic

**Fig. 1.** XRD patterns of $Gd_{55}Co_{20-x}Al_{24}Si_1Fe_x$ as-cast rods.

**Table 1**
Critical diameters Φ, supercooled liquid region $\Delta T_x$, maximum of magnetic entropy change $|\Delta S_M^{max}|$, full width at half maximum of $|\Delta S_M|$ $\delta T_{FWHM}$, Curie temperature $T_C$ and refrigerant capacity RC for $Gd_{55}Co_{20-x}Al_{24}Si_1Fe_x$ MGs under applied field of 5 T. Some values of pervious typical works are also listed for comparison.

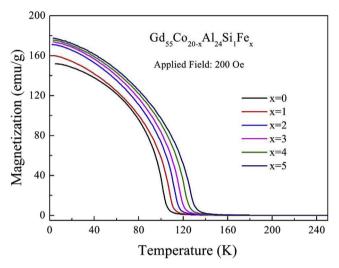| Composition | Φ (mm) | $\Delta T_x$ (K) | $T_C$ (K) | $|\Delta S_M^{max}|$ (Jkg$^{-1}$K$^{-1}$) | $\delta T_{FWHM}$ (K) | RC (Jkg$^{-1}$) | Ref. |
|---|---|---|---|---|---|---|---|
| $Gd_5Si_2Ce_{1.9}Fe_{0.1}$ | Cryst. | – | 276 | 7 | | 360 | [4] |
| $Gd_{60}Ni_{37}Co_3$ | < 1 | 15 | 135 | 10.42 | – | 860 | [23] |
| $Gd_{53}Co_{24}Al_{20}Zr_3$ | 3 | 54 | 93 | 9.4 | – | 780 | [20] |
| $Gd_{33}Er_{22}Co_{20}Al_{25}$ | 3 | – | 52 | 9.47 | – | 574 | [20] |
| $Gd_{55}Co_{20}Al_{24}Si_1$ | 5 | 74 | 101 | 8.43 | 82 | 691 | This work |
| $Gd_{55}Co_{19}Al_{24}Si_1Fe_1$ | 6 | 74 | 107 | 7.83 | 96 | 751 | This work |
| $Gd_{55}Co_{18}Al_{24}Si_1Fe_2$ | 6 | 70 | 111 | 8.05 | 100 | 805 | This work |
| $Gd_{55}Co_{17}Al_{24}Si_1Fe_3$ | 3.5 | 68 | 117 | 7.83 | 107 | 838 | This work |
| $Gd_{55}Co_{16}Al_{24}Si_1Fe_4$ | 3 | 65 | 121 | 7.55 | 112 | 845 | This work |
| $Gd_{55}Co_{15}Al_{24}Si_1Fe_5$ | 2.5 | 63 | 126 | 7.26 | 118 | 857 | This work |



**Fig. 3.** Temperature dependence of magnetization in a magnetic field of 200 Oe for $Gd_{55}Co_{20-x}Al_{24}Si_1Fe_x$ glassy alloys.
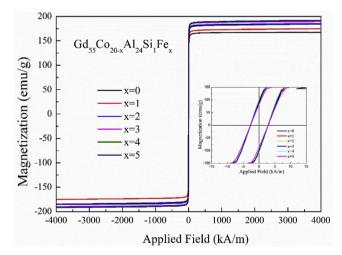


**Fig. 4.** Magnetic hysteresis loops of $Gd_{55}Co_{20-x}Al_{24}Si_1Fe_x$ melt-spun glassy ribbons at 5 K.
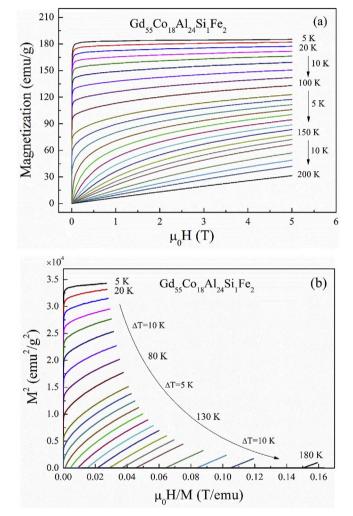


**Fig. 5.** (a) Isothermal magnetization curves of $Gd_{55}Co_{18}Al_{24}Si_1Fe_2$ glassy alloys between 5 K and 180 K under a field change of 0–5 T. (b) Corresponding Arrott plots that calculated from the isothermal magnetization curves in (a).

fields. In this work, $H_{max}$ and $H_0$ are 5 T and 0 T, respectively. Fig. 6 shows the $|\Delta S_M|$ as a function of temperature for $Gd_{55}Co_{20-x}Al_{24}Si_1Fe_x$ (x = 0, 1, 2, 3, 4 and 5) glassy ribbons for a magnetic field change of 5 T. The maximum values of $|\Delta S_M|$ are 8.43, 7.83, 8.05, 7.83, 7.55 and 7.26 J kg$^{-1}$K$^{-1}$ for the Gd-based MGs with compositions of x = 0, 1, 2, 3, 4 and 5, respectively. Although the peak temperatures shift to higher values as the Fe content increases, the effect of Fe substitution on the $|\Delta S_M|$ is not monotonic. Initially, the maximum value of $|\Delta S_M|$ slightly decreases as the Fe content increases, and reaches a minimum value of 7.83 J kg$^{-1}$K$^{-1}$ for the sample with x = 1; then the maximum value of

$|\Delta S_M|$ increases as the Fe content further increases, and reaches a maximum value of 8.05 J kg$^{-1}$K$^{-1}$ for the sample with x = 2; finally, the maximum value of $|\Delta S_M|$ clearly decreases with the further increasing of Fe content. The maximum value of $|\Delta S_M|$ obtained in this work are much larger than that of bulk amorphous Pd-based alloys (0.58 J kg$^{-1}$K$^{-1}$under a field of 5 T) [27] and Fe-and Co-based glassy ribbons (less than 2 J kg$^{-1}$ under a field of 5 T) [28].

The maximum value of $|\Delta S_M|$ and the RC are considered to be two main parameters to characterize the magnetocaloric materials [29]. For amorphous magnetocaloric materials, RC as an effective parameter for
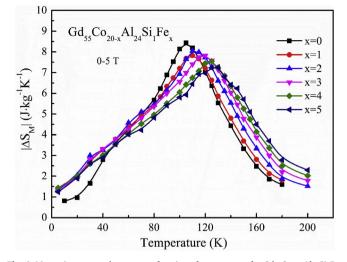
**Fig. 6.** Magnetic entropy changes as a function of temperature for $Gd_{55}Co_{20-x}Al_{24}Si_1Fe_x$ glassy samples at the magnetic field changes of 0–5 T.

characterizing refrigerant ability has been proven and widely used [1,16,17,20,23,24,30]. A compromise between the peak magnetic entropy change and the width of the peak is necessary for a reciprocating cycle [30]. The RC estimated using Gschneidner method [14] can be expressed as:

$$RC = -\Delta S_M^{max} \times \delta T_{FWHM} \qquad (2)$$

where $\delta T_{FWHM}$ presents the full width at half maximum of $|\Delta S_M|$. The $\delta T_{FWHM}$ and RC values of the alloys are calculated and presented in Table 1. As shown in Table 1 and Fig. 6, the $\delta T_{FWHM}$ obviously increases with increasing Fe content; the $\delta T_{FWHM}$ increases from 82 K for alloy with x = 0 to 118 K for alloy with x = 5. Calculated from Eq. (2), the values of RC are 691, 751, 805, 838, 845 and 857 J kg$^{-1}$ for compositions of x = 0, 1, 2, 3, 4 and 5, respectively. As shown in Table 1, the RC and GFA of the Gd-based BMGs in this work are superior to most of the previously reported glassy magnetic refrigerants [20–23], which make them promising candidates in magnetic refrigeration applications.

## 4. Discussion

The typical broad diffraction peaks in the XRD patterns for the as-cast rods indicate that the fully amorphous structure can be obtained for these Gd-based alloys.

The DSC curves for the as-cast $Gd_{55}Co_{20-x}Al_{24}Si_1Fe_x$ (x = 0, 1, 2, 3, 4 and 5) BMGs show that the $T_x$ and the peak temperature decrease as the Fe content increases. It is well known that magnetic refrigerants generally work near with their magnetic phase transition temperatures. The $T_x$ for all the $Gd_{55}Co_{20-x}Al_{24}Si_1Fe_x$ MGs are much higher than their $T_C$. Therefore, the Fe-substituted $Gd_{55}Co_{20-x}Al_{24}Si_1Fe_x$ MGs are more stable over the practical application temperature range. The existence of more than two distinct exothermic peaks for $Gd_{55}Co_{20-x}Al_{24}Si_1Fe_x$ (x = 1, 2, 3, 4 and 5) samples indicates that the crystallization process of these BMGs proceed through a multi-stage mode.

The magnetization measurements (Fig. 3) show that the $T_C$, which is strongly related to the magnetic structural stability of the material, increases from 100 K for alloy with x = 0 to 126 K for alloy with x = 5. The Fe substitution improves the magnetic exchange coupling of the metastable Gd-based MGs and thus improves the $T_C$.

The hysteresis loops measured at 5 K for the $Gd_{55}Co_{20-x}Al_{24}Si_1Fe_x$ (x = 0, 1, 2, 3, 4 and 5) glassy ribbons (Fig. 4) show that all the samples have good soft magnetic properties with negligible hysteresis and very small coercivities, which can be attribute to the weak magnetic anisotropy resulting from the structural disorder [24]. The low coercivity

indicates that the Gd-based MGs can be easily magnetised and demagnetised, and this property is favorable for magnetic refrigeration applications. The isothermal magnetization curves (Fig. 5) show that below the $T_C$, the magnetization curves increase abruptly at a rather low field and saturate rapidly; this rapid saturation suggests the fully ferromagnetic behavior of these MGs. Above the $T_C$, the increase of magnetization curves nearly becomes linear; thus, the Gd-based MGs present the characteristics of a paramagnet.

It is well known that the maximum value of $|\Delta S_M|$ is closely related to the magnetic interactions. The free electrons in transition metals act as an exchange interaction medium between 3d electrons and 4f electrons. The substitution of Fe for Co induces more unpaired 3d free electrons (Fe-3$d^6$, Co-3$d^7$), which enhances the Ruderman-Kittel-Kasuya-Yosida (RKKY) magnetic interactions that dominate the magnetic properties in rare-earth based alloys [31,32], thereby increases the exchange energy and results in a large MCE. In general, for the complicated composition caused by Fe substitution, minor Fe addition does not destruct the thermal stability of the alloys; moreover, it increases the critical diameter of the BMGs up to 6.0 mm. Meanwhile, it is distinct that the $T_C$ can be tuned easily by Fe alloying in this alloy system. Attribute to the structure disordering induced by complicated composition, and the RKKY magnetic interactions enhanced by Fe substitution, Gd-based MGs with enhanced GFA and improved magnetic performances such as raised $T_C$, wider magnetic transition temperature range, and larger RC were achieved.

It has been concluded that although the maximum value of $|\Delta S_M|$ for glassy alloys are lower than that of crystalline samples, the temperature range of the half maximum of the entropy peak is much larger; this large range enhances the refrigeration capacity of the glassy materials. Furthermore, the adiabatic temperature change is another parameter for a comparison among different MCE materials, which can be evaluated indirectly from $|\Delta S_M|$ and temperature dependence of specific heat capacity. For the Gd-based MGs, it has been reported that the maximum value of adiabatic temperature change is about 4–5 K under 5 T in the previous works [21,22,33], which is comparable with some promising magnetic refrigeration materials [34,35]. From above analysis, such excellent GFA and large RC make these $Gd_{55}Co_{20-x}Al_{24}Si_1Fe_x$ MGs attractive candidates for magnetic refrigeration applications.

## 5. Conclusion

In this work, excellent GFA and MCE were observed in $Gd_{55}Co_{20-x}Al_{24}Si_1Fe_x$ (x = 0, 1, 2, 3, 4 and 5) MGs. Bulk glassy alloys with diameters up to 6.0 mm were formed by copper mold casting technology. The effect of Fe substitution for Co on the improvement of GFA and magnetocaloric properties of Gd-based MGs were investigated. The results can be summarized as follows:

(1) The introduction of Fe improved the disorder degree, leading to a larger critical diameter of the alloys. With 1 to 2 at% Fe addition, BMGs with diameter of 6.0 mm were fabricated.

(2) The magnetization measurements showed that the $T_C$ increased from 100 K for alloy with x = 0 to 126 K for alloy with x = 5. The increase in the $T_C$ with increasing Fe content could be attribute to the increase of magnetic exchange coupling in the amorphous phase. The Gd-based MGs have good soft magnetic properties with negligible hysteresis and small coercivities.

(3) The large $\delta T_{FWHM}$ of 100 K, maximum value of $|\Delta S_M|$ of 8.05 J kg$^{-1}$K$^{-1}$, and corresponding large RC of 805 J kg$^{-1}$ under applied field of 5 T were obtained for the $Gd_{55}Co_{18}Al_{24}Si_1Fe_2$ glassy alloy. Such high GFA of novel Gd-based MGs with large MCE make them attractive candidates for magnetic refrigeration applications in the future.

## Acknowledgements

## References

[1] V. Franco, J. Blázquez, B. Ingale, A. Conde, Annu. Rev. Mater. Res. 42 (2012) 305–342.
[2] O. Gutfleisch, M.A. Willard, E. Brück, C.H. Chen, S. Sankar, J.P. Liu, Adv. Mater. 23 (2011) 821–842.
[3] Q. Luo, B. Schwarz, N. Mattern, J. Shen, J. Eckert, AIP Adv. 3 (2013) 032134.
[4] V. Provenzano, A.J. Shapiro, R.D. Shull, Nature 429 (2004) 853–857.
[5] V.K. Pecharsky, K.A. Gschneidner Jr., Phys. Rev. Lett. 78 (1997) 4494–4497.
[6] Z.B. Guo, Y.W. Du, J.S. Zhu, H. Huang, W.P. Ding, D. Feng, Phys. Rev. Lett. 78 (1997) 1142–1145.
[7] F.X. Hu, B.G. Shen, J.R. Sun, Appl. Phys. Lett. 76 (2000) 3460–3462.
[8] F.X. Hu, B.G. Shen, J.R. Sun, Z.H. Cheng, G.H. Rao, X.X. Zhang, Appl. Phys. Lett. 78 (2001) 3675–3677.
[9] O. Tegus, E. Brück, K. Buschow, F. De Boer, Nature 415 (2002) 150–152.
[10] Y. Zhang, Q. Zheng, W.X. Xia, J. Zhang, J. Du, A.R. Yan, Scr. Mater. 104 (2015) 41–44.
[11] P. Gębara, J. Kovac, Mater. Des. 129 (2017) 111–115.
[12] W.M. Yang, J.T. Huo, H.S. Liu, J.W. Li, L.J. Song, Q. Li, L. Xue, B.L. Shen, A. Inoue, J. Alloys Comp. 684 (2016) 29–33.
[13] Q. Li, P.P. Cai, B.L. Shen, A. Makino, A. Inoue, J. Magn. 16 (2011) 440–443.
[14] K.A. Gschneidner Jr., V.K. Pecharsky, Annu. Rev. Mater. Sci. 30 (2000) 387–429.
[15] Q. Li, B.L. Shen, IEEE Trans. Magn. 47 (2011) 2490–2493.
[16] J.T. Huo, L.S. Huo, H. Men, X.M. Wang, A. Inoue, J.Q. Wang, C.T. Chang, R.W. Li, Intermetallics 58 (2015) 31–35.
[17] F.X. Qin, N.S. Bingham, H. Wang, H.X. Peng, J.F. Sun, V. Franco, S.C. Yu, H. Srikanth, M.H. Phan, Acta Mater. 61 (2013) 1284–1293.
[18] W.M. Yang, J.W. Li, H.S. Liu, C.C. Dun, H.L. Zhang, J.T. Huo, L. Xue, Y.C. Zhao, B.L. Shen, L.M. Dou, A. Inoue, Intermetallics 49 (2014) 52–56.
[19] A. Smith, C.R. Bahl, R. Bjørk, K. Engelbrecht, K.K. Nielsen, N. Pryds, Adv. Energy Mater. 2 (2012) 1288–1318.
[20] Q. Luo, D.Q. Zhao, M.X. Pan, W.H. Wang, Appl. Phys. Lett. 89 (2006) 081914-3.
[21] F. Yuan, J. Du, B.L. Shen, Appl. Phys. Lett. 101 (2012) 032405-4.
[22] Z. Li, D. Ding, L. Xia, Intermetallics 86 (2017) 11–14.
[23] Y.F. Ma, B.Z. Tang, L. Xia, D. Ding, Chin. Phys. Lett. 33 (2016) 126101–126104.
[24] Q. Luo, W.H. Wang, J. Non-Cryst Solids 355 (2009) 759–775.
[25] S.K. Banerjee, Phys. Lett. 12 (1964) 16–17.
[26] E. Brück, K.H.J. Buschow (Ed.), Handbook of Magnetic Materials, vol. 17, North-Holland, Amsterdam, 2008, p. 235.
[27] T.D. Shen, R.B. Schwarz, J.Y. Coulter, J.D. Thompson, J. Appl. Phys. 91 (2002) 5240–5245.
[28] M.X. Zhang, J.W. Li, F.L. Kong, J. Liu, Intermetallics 59 (2015) 18–22.
[29] V. Franco, C.F. Conde, A. Conde, L.F. Kiss, Appl. Phys. Lett. 90 (2007) 052509-3.
[30] M.E. Wood, W.H. Potter, Cryogenics 25 (1985) 667–683.
[31] K. Yosida, Phys. Rev. 106 (1957) 893–898.
[32] M.A. Ruderman, C. Kittel, Phys. Rev. 96 (1954) 99–102.
[33] L. Xia, M.B. Tang, K.C. Chan, Y.D. Dong, J. Appl. Phys. 115 (2014) 223904–223905.
[34] V.A. Chernenko, J.M. Barandiaran, J.R. Fernandez, D.P. Rojas, J. Gutierrez, P. Lazpitaa, I.J. Orue, Magn. Magn. Mater 324 (2012) 3519–3523.
[35] Z.W. Wang, P. Yu, Y.T. Cui, L. Xia, J. Alloy Comp. 658 (2016) 598–602.